Article published online: 2024-07-15

Original Article

Discovery of a Novel Benzimidazole Necroptosis Inhibitor from an In-House Compound Library

Yu Zou[1#] Yue Chai[2#] Hongming Shao[2] Shuyu Wang[3] Ruilin Hou[3] Runhui Liu[2] Linjing Zhao[1*] Chunlin Zhuang[2,4*]

[1] College of Chemistry and Chemical Engineering, Shanghai University of Engineering Science, Shanghai, People's Republic of China
[2] School of Pharmacy, Second Military Medical University, Shanghai, People's Republic of China
[3] School of Pharmacy, Ningxia Medical University, Yinchuan, People's Republic of China
[4] The Center for Basic Research and Innovation of Medicine and Pharmacy (MOE), School of Pharmacy, Second Military Medical University, Shanghai, People's Republic of China

Address for correspondence Linjing Zhao, PhD, College of Chemistry and Chemical Engineering, Shanghai University of Engineering Science, 333 Longteng Road, Shanghai 201620, People's Republic of China (e-mail: ljzhao@sues.edu.cn).

Chunlin Zhuang, PhD, School of Pharmacy, Second Military Medical University, 325 Guohe Road, Shanghai 200433, People's Republic of China (e-mail: zclnathan@163.com).

Pharmaceut Fronts

Abstract

Necroptosis, a caspase-independent regulated cell death, is primarily mediated by the serine/threonine kinases RIPK1 and RIPK3, and the mixed lineage kinase domain-like protein (MLKL). Targeting necroptosis is a validated therapeutic strategy for various diseases. We screened compound **1**, a novel benzimidazole-based necroptosis inhibitor, from our in-house compound library. We assessed its inhibitory roles and mechanisms in blocking HT-29 cell necroptosis. HT-29 cells were treated with pan caspase inhibitor Z-VAD-FMK + Smac mimetic (TSZ), or Z-VAD-FMK + cycloheximide (TCZ), then with tumor necrosis factor α (TNFα) to induce necroptosis *in vitro*. Prior to stimulation, cells were exposed to compound **1**. GSK'843 served as a control drug. HT-29 cells were treated with TNFα + Smac mimetic (TS) or TNFα + cycloheximide (TC) to induce apoptosis *in vitro*. Cell viability, cell death, and necroptotic cells were evaluated by luminescence-based CellTiter-Lumi assay or flow cytometry. Western blots, immunoprecipitation, and KINOMEscan technology were used to assess RIPK1, RIPK3, and MLKL's involvement in compound **1**'s mechanisms. Compound **1**'s roles in mouse TNFα induced systemic inflammatory response syndrome (SIRS) in mice were also investigated by assessing body temperature, mouse survival rate, and interleukin (IL)-β and IL-6 levels in respective tissues. We found that necroptosis triggered by TSZ or TCZ was effectively mitigated by compound **1**, showing a dose-responsive inhibition, and it could protect mice from TNF-induced SIRS. The mechanism study showed that compound **1** could interact with RIPK1, inhibiting RIPK1 phosphorylation activation to block necrosome formation in necroptotic cells. In summary, compound **1** is a promising lead compound for developing treatments targeting diseases associated with necroptosis.

Keywords
- benzimidazole
- necroptosis
- inhibitors
- screening
- SIRS

[#] *These authors contributed to this work equally.*

received
May 26, 2024
accepted
June 18, 2024

DOI https://doi.org/10.1055/s-0044-1788077.
ISSN 2628-5088.

Georg Thieme Verlag KG, Rüdigerstraße 14, 70469 Stuttgart, Germany

Introduction

Necroptosis, a form of programmed cell death, operates independently of caspases and is regulated by various death receptors.[1] Characterized by cell swelling, membrane rupture, and release of endogenous adjuvants, it ultimately leads to cell death.[2,3] The necroptosis signaling cascade can be triggered by multiple stimuli, including tumor necrosis factor (TNF), CD95/Fas,[4] toll-like receptor 3/4,[5] DNA-dependent activator of interferon regulatory factors (DLM1 or ZBP1),[6] and lipopolysaccharide.[7] The TNFα-mediated necroptotic mechanism, a classic pathway, has been extensively studied.

In the TNFα-triggered necroptosis pathway, cellular responses begin when TNFα molecules interact with cell membrane-located TNF receptor 1 (TNFR1). This interaction triggers a conformational shift in TNFR1, recruiting TNFR1 death-related domain protein (TRADD), TNF receptor 2 (TRAF2), cellular inhibitor of apoptosis proteins 1/2 (cIAP1/2), and serine/threonine kinase RIPK1, initiating a molecular cascade and forming Complex I.[8,9] Within this complex, RIPK1 undergoes ubiquitination by E3 ligase and cIAP1/2, activating the NF-κB signaling pathway and promoting cell survival.[10] However, when cIAP1/2 is inhibited by a second mitochondria-derived caspase activator (Smac) or Smac mimetic chemical, RIPK1 ubiquitination is prevented. Consequently, Complex I releases TNFR2 and recruits Fas-associated death domain protein (FADD) to assemble Complex II. Within Complex II, FADD activates caspase 8, promoting apoptosis.[11,12] When caspase 8 activity is suppressed by the broad-spectrum caspase inhibitor Z-VAD-FMK,[13] RIPK1 and RIPK3 interact through the RIP homotypic interaction motif domain and form heterodimer filamentous structures, known as necrosomes,[14,15] activating the necroptosis pathway. Upon phosphorylation, RIPK3 becomes active and recruits its downstream substrate, MLKL, phosphorylating it.[16,17] This leads to MLKL aggregation and concentration at the plasma membrane. Subsequently, oligomerized MLKL disrupts necrotic cells' plasma membranes.[18,19] This process activates inflammasomes and stimulates the release of damage-associated molecular patterns (DAMPs), initiating a severe inflammatory reaction in the surrounding tissue. The initiation of this inflammatory cascade depends on the activation of the RIPK1 kinase, which is fundamental for necrosome assembly and necroptosis mediation. It has been reported that cells can be protected from TNFα-induced necroptosis by inhibiting RIPK1 kinase activation through gene knockout or small-molecule inhibitors targeting RIPK1 kinase.[20] Therefore, discovering innovative compounds capable of inhibiting RIPK1 kinase activity presents a promising avenue for developing potential therapeutic strategies to combat diseases associated with necroptosis.

Early in 2005, Yuan's group discovered the first small-molecule inhibitor for RIPK1, Nec-1 (►**Fig. 1**), by screening a 15,000-compound library.[21] This compound had excellent anti-necroptotic activity, with an EC_{50} of 0.49 μmol/L and a high RIPK1 selectivity. However, pharmacokinetic studies revealed a significant limitation: a very short half-life ($t_{1/2}$ < 5 minutes), which resulted in poor druggability. Further investigations also highlighted a narrow structure–activity relationship for this scaffold.[21,22] Despite these challenges, the discovery of Nec-1 significantly advanced the exploration of the necroptosis pathway, enhancing our understanding of its mechanisms and stimulating the development of related compounds. RIPA-56 emerged as a potent anti-necroptotic compound (EC_{50} = 28 nmol/L in HT-29 cells) with a high selectivity toward RIPK1 (IC_{50} = 13 nmol/L). Notably, this compound demonstrated a significant reduction in mortality and multi-organ damage induced by TNFα in a murine model of systemic inflammatory response syndrome (SIRS).[23] GlaxoSmithKline has pioneered an array of RIPK1 inhibitors, including the dihydropyrazole derivative GSK'963,[24] GSK'547,[25] and the representative benzoxazepinone derivative GSK'772.[26] GSK'772 has undergone clinical trials for various inflammatory disorders, such as ulcerative colitis, rheumatoid arthritis, and psoriasis.[27] Another noteworthy RIPK1 inhibitor is SAR443060 (previously known as

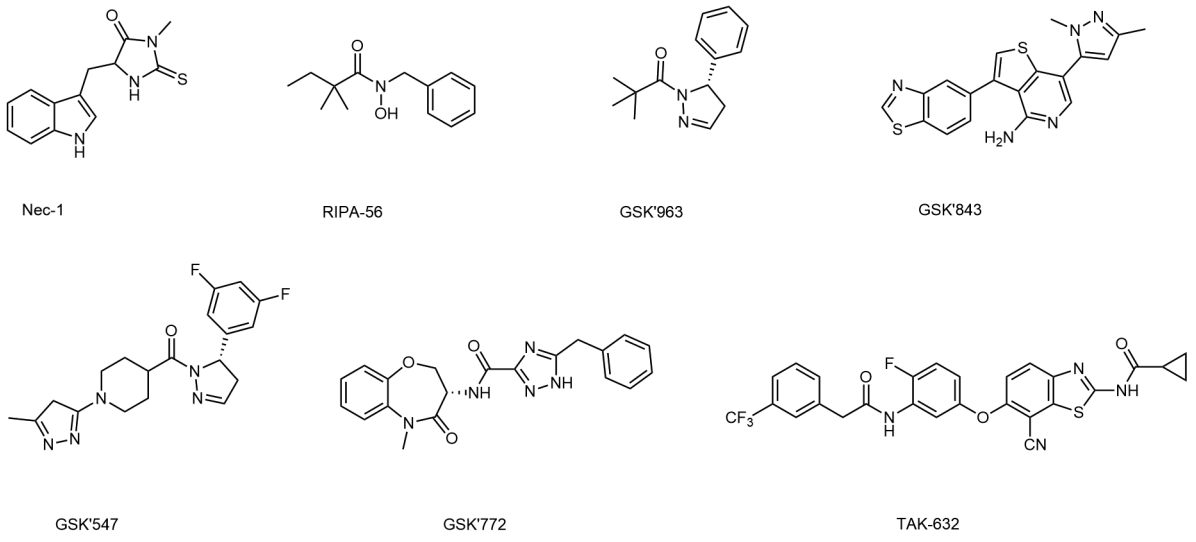

Fig. 1 The typical necroptosis inhibitors targeting RIPK1/3 and the benzothiazole compound TAK-632.

DNL747). This selective RIPK1 inhibitor, whose molecular structure remains confidential, is characterized by its oral bioavailability and ability to cross the blood–brain barrier. It functions as a reversible inhibitor of RIPK1 and has been utilized in clinical settings for the treatment of conditions including amyotrophic lateral sclerosis and Alzheimer's disease.[28] GSK'843 has been reported as a RIPK3 inhibitor, contributing to inflammation research.[5,29] In addition, our group has developed a series of benzothiazole compounds targeting RIPK1/RIPK3, such as TAK-632 and its analogs.[30–35] These compounds are specifically designed to target the kinase domain of RIPK1, thereby exerting their anti-necroptosis effects; however, they have been limited by the types of scaffolds used and have not yet successfully advanced into clinical applications. Therefore, the development of novel types of compounds targeting the necroptosis pathway remains an urgent requirement.

In this study, we screened our modest in-house library, which consists of 78 compounds, to assess their ability to inhibit TNFα-trigged necroptotic cell death in HT-29 cells. Compound **1** demonstrated potential anti-necroptosis activity in both TSZ/TCZ-induced necroptosis models. The mechanism underlying the action of this compound will be investigated. Additionally, we will assess the efficacy of this compound in a mouse model of SIRS.

Material and Methods

Material

The HT-29 cells used in this study were sourced from our in-house laboratory cell bank. The high-glucose Dulbecco's Modified Eagle's Medium (DMEM) and the Penicillin-Streptomycin (100 ×) solution, along with the phosphate-buffered saline (PBS), were procured from Bio-Channel, based in Nanjing, China. Fetal bovine serum (FBS) was obtained from Biological Industries (Heit Haemek, Israel). The recombinant mouse/human TNFα was obtained from Novo-protein (Shanghai, China). The pan-caspase inhibitor Z-VAD-FMK (catalog number T6013) was purchased from TargetMol, United States. An Smac mimetic compound (HY-15989) was sourced from MedChemExpress (Monmouth Junction, New Jersey, United States). Lastly, cycloheximide (catalog number 66–81–9) was procured from AccuStandard (Connecticut, United States).

For the immunoblotting assays conducted in this study, we employed a range of antibodies sourced from commercial suppliers. These included the anti-RIPK1 antibody (Abcam, catalog number ab3493S, used at a dilution of 1:1,000), the anti-human phospho-RIPK1 antibody (Abcam, catalog number ab65746S, used at a dilution of 1:1,000), and the anti-human phospho-RIPK3 antibody (Abcam, catalog number ab209384, used at a dilution of 1:1,000). We also used the anti-human MLKL antibody (Abcam, catalog number ab184718, used at a dilution of 1:1,000), the antihuman phospho-MLKL antibody (Abcam, catalog number ab91689S, used at a dilution of 1:1,000), and the anti-GAPDH antibody (Proteintech, United States, used at a dilution of 1:10,000), which served as a loading control.

The Annexin V-FITC/propidium iodide (PI) Apoptosis Detection Kit, integral to our study, was procured from MedChemExpress (United States). We also utilized the CellTiter-Glo Luminescent Cell Viability Assay Kit (C0065XL), sourced from Beyotime (Shanghai, China), and the BCA protein assay Kit, obtained from Biosharp (Hefei, China).

Cell Culture

HT-29 cells were cultured in DMEM supplemented with 10% FBS (v/v), 1% *L*-glutamine (v/v), and 100 U/mL penicillin/streptomycin. These cells were maintained in a humidified chamber at 37°C, under an atmosphere containing 5% CO_2. For all experiments, we ensured that cells were harvested from culture mediums that were in the exponential phase of growth, thereby ensuring optimal cellular conditions for our investigations.

Necroptosis and Apoptosis Induction and Treatment

Necroptosis was triggered by pretreatment with Z-VAD-FMK (20 μmol/L), in combination with either Smac mimetic (10 nmol/L) or cycloheximide (20 μmol/L) for a duration of 30 minutes. This was followed by an application of TNFα (20 ng/mL) for a period of either 9 hours (in the case of HT-29 cells, referred to as TSZ when combined with Smac mimetic) or 12 hours (referred to as TCZ when combined with cycloheximide). However, apoptosis was triggered by exposing the cells to TNFα (20 ng/mL) in conjunction with Smac mimetic at a concentration of 60 nmol/L (referred to as TS) or cycloheximide at a concentration of 120 μmol/L (referred to as TC) for a period of 24 hours.[30,33,34,36,37] Compound **1** and the control drug GSK'843 were introduced to the cells subjected to one of the aforementioned treatment regimens at designated concentrations for 9, 12, and 24 hours.

Necroptosis and Apoptosis Assessment

The necroptotic phenotype of the compound was examined using phase contrast microscopy. Following this, the CellTiter-Glo Luminescent Cell Viability Assay Kit was employed to determine cell viability, with luminescence measurements recorded on a SpectraMax M5e microplate reader, as per the manufacturer's guidelines. Cell death was assessed via fluorescence-activated cell sorting. The cells were treated with either an Annexin V-FITC/PI Apoptosis Detection Kit or stained solely with PI. After the supernatant was collected, the cells underwent trypsin treatment (0.25% EDTA, Bio-Channel, Nanjing, China) and were incubated at 37°C for 2 minutes to enable detachment. This was followed by two rounds of washing with ice-cold PBS to cleanse the cells. The cells were then centrifuged at 1,000 rpm for 2 minutes to form pellets. After centrifugation, the cell pellets were washed once more with ice-cold PBS to ensure purity. For necroptosis analysis, the cells were resuspended in a solution of 300 μL of ice-cold PBS supplemented with 2 μL of PI solution. In contrast, for apoptosis assessment, the cells were resuspended in 300 μL of Annexin V-FITC buffer, which included 2 μL of PI solution and 2 μL of Annexin V-FITC

solution. Both resuspensions were kept at room temperature for a minimum of 15 minutes to facilitate staining. The proportions of PI-negative cells (viable cells), Annexin V-FITC(−)/PI(−)-cells (viable cells in the lower left quadrant), and Annexin V-FITC(+)/PI(+) cells (apoptotic cells in the upper right quadrant) were quantified using a Becton Dickinson Biosciences FACSCalibur.[30]

Western Blots

HT-29 cells were subjected to a 6-hour exposure to TSZ and compound **1**. Following this treatment, proteins were extracted using a nonidet P-40 lysis buffer, which was enhanced with 1% protease inhibitor, 1% phosphatase inhibitor, and 1% PMSF (all sourced from Beyotime Biotechnology, China) to prevent protein degradation and maintain phosphorylation states. Protein quantification was conducted using the BCA protein assay Kit (Biosharp, China), adhering to the manufacturer's instructions. The isolated protein samples were then dissolved in SDS-PAGE (sodium dodecyl sulfate–polyacrylamide gel electrophoresis) loading buffer and heated to 100°C for 10 minutes to denature the proteins. The denatured protein samples were subsequently separated through SDS-PAGE, and the resolved proteins were transferred onto nitrocellulose (NC) membranes (catalog number 15596026, Beyotime, China). To block nonspecific binding sites, the NC membranes were pretreated with a 5% skim milk solution for 1 hour. Primary antibodies, specific to the proteins of interest, were diluted to a concentration of 1:1,000 in 5% skim milk. The membranes were then incubated overnight at 4°C with these primary antibodies. Following this incubation period and subsequent washing, the membranes were exposed to appropriately diluted secondary antibodies (goat anti-rabbit, catalog number D21109–35, donkey anti-mouse, catalog number D21109–15, LI-COR, United States) at a ratio of 1:10,000 in a 5% skim milk solution for 1 hour at room temperature to facilitate detection. Finally, the protein bands were analyzed using the Image Studio Ver 5.2 system (LI-COR, Lincoln, United States), and gray values were evaluated using Image J.

Immunoprecipitation Assay

HT-29 cells were treated with compound **1** and TSZ for a duration of 6 hours. Posttreatment, the cells were washed twice with ice-cold PBS to remove residual media components. The cells were then collected using a cell scraper and lysed in a nonidet P-40 buffer (Beyotime, China), in accordance with Western blot protocols. The lysed cell suspension was centrifuged to separate soluble proteins from cellular debris. The supernatant was collected, and protein concentrations were determined using a standard assay method. The supernatant was then treated with an anti-RIPK1 antibody and incubated at 4°C for 24 hours to facilitate the specific precipitation of RIPK1 protein complexes. The immunocomplex was immunoprecipitated using Protein A/G Agarose beads (Life Technologies). The mixture was further incubated with the beads at 4°C for an additional 24-hour period to ensure the capture of the antibody–antigen complexes. Following this, the beads were extensively washed with PBS to remove unbound proteins. The bound proteins were eluted from the beads by boiling them in SDS-PAGE loading buffer. The precipitated samples obtained were then resolved on a 10% SDS-PAGE gel and analyzed via the aforementioned Western blots (immunoblotting).

In Vitro Kinase Assay

The interaction between compound **1** and the RIPK1/3 kinase was assessed using KINOMEscan technology (Eurofins, United States). Initially, T7 phage strains expressing the RIPK1 kinase were labeled with a DNA tag for subsequent detection via quantitative polymerase chain reaction (qPCR). The binding assay involved mixing the kinase, ligand-coupled affinity beads, and compound **1** in a binding buffer composed of 20% SeaBlock, 0.17 × PBS, 0.05% Tween 20, and 6 mmol/L dithiothreitol. Compound **1** was prepared at a stock concentration of 5 mmol/L in 100% DMSO. The K_d values were measured using an 11-point dilution series of the compound, with each point representing a threefold dilution and three control points containing only DMSO. This ensured a comprehensive assessment of the compound's binding affinity across a wide concentration range. The compounds were added directly to the assay mixture, maintaining the final DMSO concentration at 0.9% to minimize any solvent effects on the assay. All reactions were conducted in a polypropylene 384-well plate format. The assay was performed with the plates incubated at room temperature with constant shaking for 1 hour to facilitate binding. After incubation, the affinity beads were washed with a wash buffer (1 × PBS, 0.05% Tween 20) to remove any nonspecifically bound kinase or compound. The beads were then resuspended in an elution buffer (1 × PBS, 0.05% Tween 20, 0.5 µmol/L nonbiotinylated affinity ligand) and incubated at room temperature for 30 minutes with shaking. The levels of the eluted kinase were subsequently quantified by qPCR by Eurofins.

Drug Affinity-Responsive Target Stability

Upon reaching the desired density, HT-29 cells were seeded in a 10-cm culture plate. The cells were then harvested by scraping them into a pre-chilled lysate buffer, followed by a 15-minute lysis on ice. After centrifugation and quantification, the lysates were incubated at 4°C with compound **1** (300 µmol/L) and DMSO with shaking for 2 hours. This was followed by digestion with 0.1, 0.067, and 0.05% pronase for 30 minutes at room temperature. The digestion process was terminated by heating the samples in an SDS-PAGE loading buffer. The protein samples were then separated on a 10% PAGE-SDS gel and subsequently analyzed via immunoblotting.[30,38]

mTNF-Induced SIRS Animal Model and Treatment

In the investigation of TNFα-induced SIRS, male C57BL/6 J mice, aged between 6 and 8 weeks, were obtained from the Shanghai Institute of Family Planning Science (Shanghai, China). The animals were housed in a sterile environment with a regulated temperature range of 22 to 27°C and relative humidity levels between 35 and 65%. Compound **1** was formulated in endotoxin-free PBS, supplemented with 13%

DMSO and 35% PEG400. Mice that had fasted overnight were randomly assigned to different groups ($n = 12$): a vehicle control group and three drug-treated groups. Mice in the drug-treated groups were administered 100, 75, and 50 mg/kg of compound **1** via intraperitoneal injection (i.p.) in 300 µL. Two hours later, mouse TNFα (mTNFα) was injected. mTNFα was prepared in endotoxin-free PBS at an appropriate dilution and administered via intravenous injection (i.v.; 50 µg/kg, 200 µL). Z-VAD-FMK was administered via i.p. at a dosage of 150 µg, formulated in PBS with 13% DMSO and 35% PEG400, 15 minutes before and followed by a 50 µg dose 45 minutes after mTNFα treatment. Body temperature was continuously monitored using an electronic thermometer for accurate and real-time measurements. The survival rate of the mice within 20 hours was analyzed using GraphPad 8.0. At the end of the experiment, tissues were collected from anesthetized mice, and the levels of interleukin (IL)-1β and IL-6 in the tissue samples were determined using an IL-1β/IL-6 ELISA Kit (Invitrogen Thermo Fisher Scientific, United States). The SIRS model was conducted in accordance with reported studies.[30,39,40]

Date and Statistical Analysis

Data were presented as mean ± standard deviation of at least three parallels. A one-way ANOVA was used to assess the differences among various groups. Survival data were evaluated using a log-rank test, also known as the Mantel–Cox test. All statistical analyses were performed using GraphPad Prism software, version 8.0. A p-value of less than 0.05 was set as the criterion for statistical significance, indicating a reliable effect or difference between the compared groups.

Results

Identification of Compound 1 as a Novel Necroptosis Inhibitor

A library of 78 compounds was screened for their efficacy in inhibiting TNFα-induced necroptosis following a 30-minute pretreatment with selected compounds, as per our previous research.[30,33–37] Cell viability was quantified using a luminescence-based assay. The concentration of the compound was set at 100 µmol/L, and GSK'843 was selected as the positive control. Compounds that maintained cell viability higher than 45% compared with untreated groups were identified as hits (►**Fig. 2A**) for further study. Interestingly, five compounds (**1**, **2**, **3**, **11**, **12**; ►**Fig. 2B**, **E**) met the criteria. Subsequently, HT-29 cells were exposed to these five identified compounds, along with GSK'843, each at a dosage of 80 µmol/L. Cell survival was evaluated through flow cytometry analysis, utilizing PI staining. Among the hits, Compound **1**, bearing a benzimidazole scaffold, demonstrated the highest potency at a concentration of 80 µmol/L (►**Fig. 2C**, **D**), comparable to the positive control compound GSK'843.

Subsequently, the potency of compound **1** underwent further validation. In the TSZ-induced necroptosis model using HT-29 cells, compound **1** demonstrated a dose-dependent capability to inhibit necroptotic cell death (►**Fig. 3A**). However, its efficacy was significantly lower than that of GSK'843 at low concentrations (10 and 20 µmol/L). Phase contrast microscopy provided additional insights, revealing that while normal cells have an intact cell membrane, regular shape and size, and clear cell boundaries, TSZ-induced necroptotic cells are characterized by cellular enlargement and breaching of the plasma membrane. Compound **1** was able to mitigate the necroptotic phenotype (►**Fig. 3B**). In the HT-29 necroptosis model induced by TCZ (►**Fig. 3C**, **D**), compound **1** protected HT-29 cells from necroptotic cell death in a dose-dependent manner. Interestingly, an assay for apoptosis induced by TS (►**Fig. 3E**, **F**) or TC (►**Fig. 3G**, **H**) showed that the protective effect of compound **1** was not apparent in HT-29 cells at the indicated concentrations.[30,33] These findings suggest that compound **1** specifically targets and inhibits the necroptosis pathway.

Compound 1 Blocked Necroptosis through the Inhibition of RIPK1 Phosphorylation

We further investigated the anti-necroptotic mechanism of compound **1**. The impact of compound **1** on the phosphorylation of RIPK1, RIPK3, and MLKL was evaluated in the TSZ-treated HT-29 cell necroptosis model. A dose range of 20 to 80 µmol/L was selected based on previous *in vitro* assays focused on anti-necroptosis. As a result, compound **1** significantly reduced the activation and phosphorylation of RIPK1 (p-S166) at 20 µmol/L, exhibiting a pronounced dose-dependent effect. The phosphorylation of RIPK3 (p-S227) and MLKL (p-S358) was also inhibited in a dose-dependent manner (►**Fig. 4A**, **D–F**). In the time-dependent assay, the evaluated time points were 2, 4, and 6 hours as referred to in previous studies.[30] At a concentration of 80 µmol/L, compound **1** completely inhibited the phosphorylation of RIPK1 at 6 hours, leading to subsequent inhibition of the phosphorylation of RIPK3 and MLKL compared with the model group (►**Fig. 4B**, **G–I**). We subsequently assessed the assembly of necrosomes in HT-29 cells treated with compound **1**. Compound **1** was found to effectively prevent the formation of necrosomes, a critical interaction between RIPK1 and RIPK3, which was induced by TSZ at a concentration of 80 µmol/L (►**Fig. 4C**). These results suggested that compound **1** is a potential necroptosis inhibitor that could prevent necrosome formation through the inhibition of RIPK1 phosphorylation.

We further explored whether compound **1** functions as a direct kinase inhibitor targeting RIPK1 and/or RIPK3. Initially, we used recombinant RIPK1 and RIPK3 proteins to measure the kinase activity *in vitro* using the KINOMEscan assay. Compound **1** was found to inhibit the kinase activity of RIPK1 at a high concentration of 100 µmol/L (70% at 100 µmol/L), consistent with the *in vitro* cell activity. However, it showed no inhibitory activity against RIPK3 kinase at the indicated concentrations (►**Fig. 5A**, **B**). Subsequently, we performed a Drug Affinity Response Target Stability (DARTS) assay, which relies on the reduced sensitivity of the target protein to protease after drug binding.[38] We found that in cell extracts incubated with compound **1**, RIPK1 was protected against 0.01% protease digestion, while RIPK3 remained undetected (►**Fig. 5C**). In conclusion, compound **1** could interact with RIPK1 and inhibit RIPK1 phosphorylation activation to block necrosome formation in necroptotic cells.

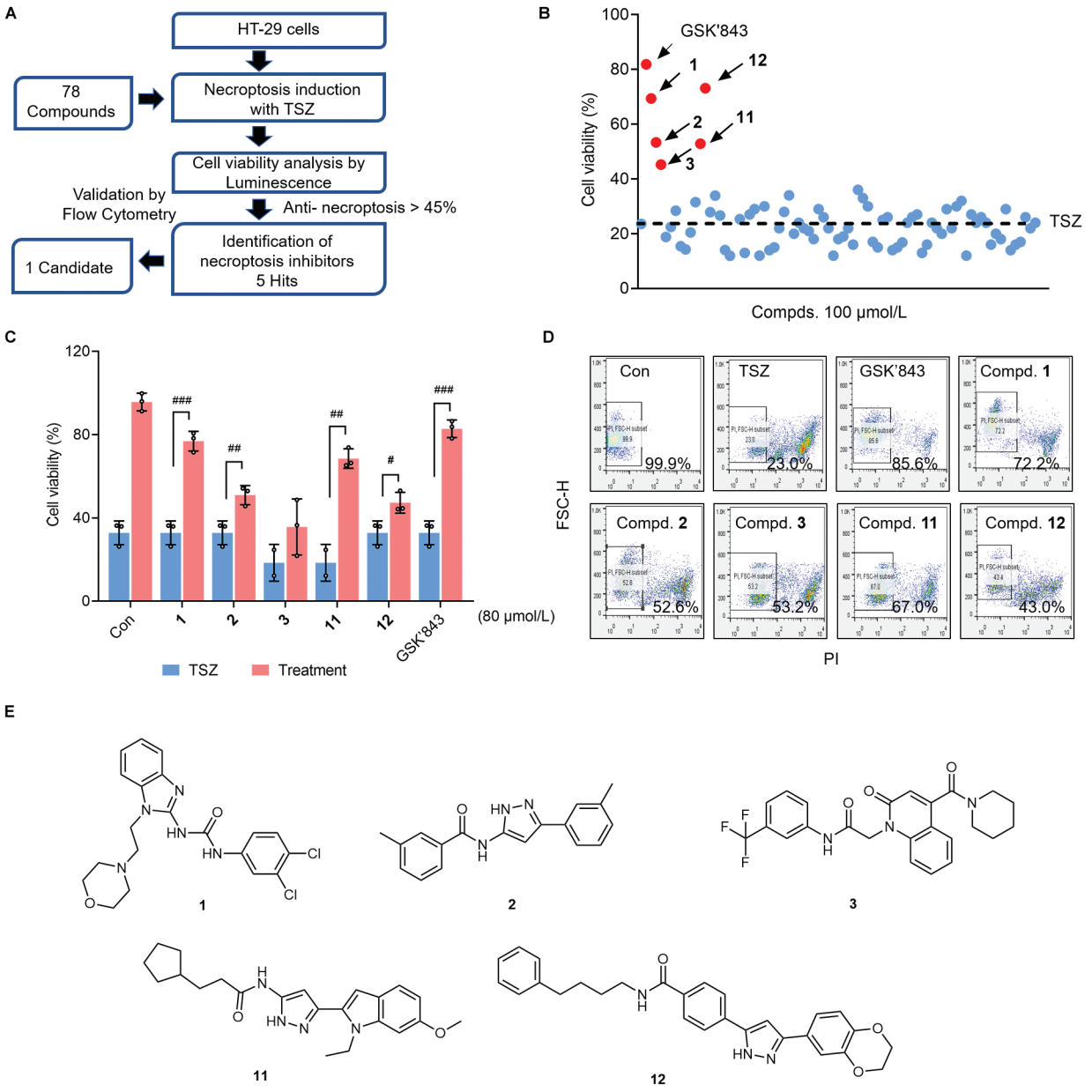

Fig. 2 Identification of novel necroptosis inhibitors. (**A**) Diagrammatic representation of the drug screening process. (**B**) Identification of a necroptosis inhibitor via cellular screening of an in-house compound library. HT-29 cells were preincubated with each compound at a concentration of 100 μmol/L for 30 minutes before stimulation with TSZ for 9 hours to trigger cell death. Cell viability was assessed using the luminescence-based CellTiter-Lumi assay, with the data normalized to the viability of the untreated control group. (**C, D**) HT-29 cells were pretreated with 5 hits (80 μmol/L) for 30 minutes subsequently challenged with TSZ for 9 hours, and then stained with PI. Viable cells (PI-negative cells) were analyzed via flow cytometry. $^{\#}p < 0.05$, $^{\#\#}p < 0.01$, $^{\#\#\#}p < 0.001$ versus stimulation without compound **1**. (**E**) Structures of the 5 hits.

Compound 1 Alleviated the Effects of TNF-Induced SIRS in Mice

We then proceeded to determine if compound **1** could mitigate inflammation driven by RIP kinase *in vivo* by examining its effects in the TNF-induced SIRS model. Compound **1** (100, 75, and 50 mg/kg) was administered i.p. 2 hours prior to the i.v. administration of mTNFα. Necroptosis-released DAMPs could activate inflammatory signaling pathways, and symptoms such as hypothermia and death in mice are characteristics of SIRS. As depicted in ►**Fig. 6A** and **6B**, compound **1** significantly protected mice from TNF-induced hypothermia and death. The survival rates were notably increased to 90% at dosages of 75 and 100 mg/kg. Furthermore, compound **1** reduced the levels of IL-1β (►**Fig. 6C**) in heart, liver, spleen, lung, and gut tissues, and IL-6 (►**Fig. 6D**) in heart, liver, spleen, lung, kidney, gut, and brain tissues induced by mTNFα. Collectively, these findings illustrate that compound **1** attenuates TNF-induced SIRS in a living organism.

Discussion

Necroptosis plays a crucial role in numerous human inflammatory diseases.[1] Therefore, the development of novel

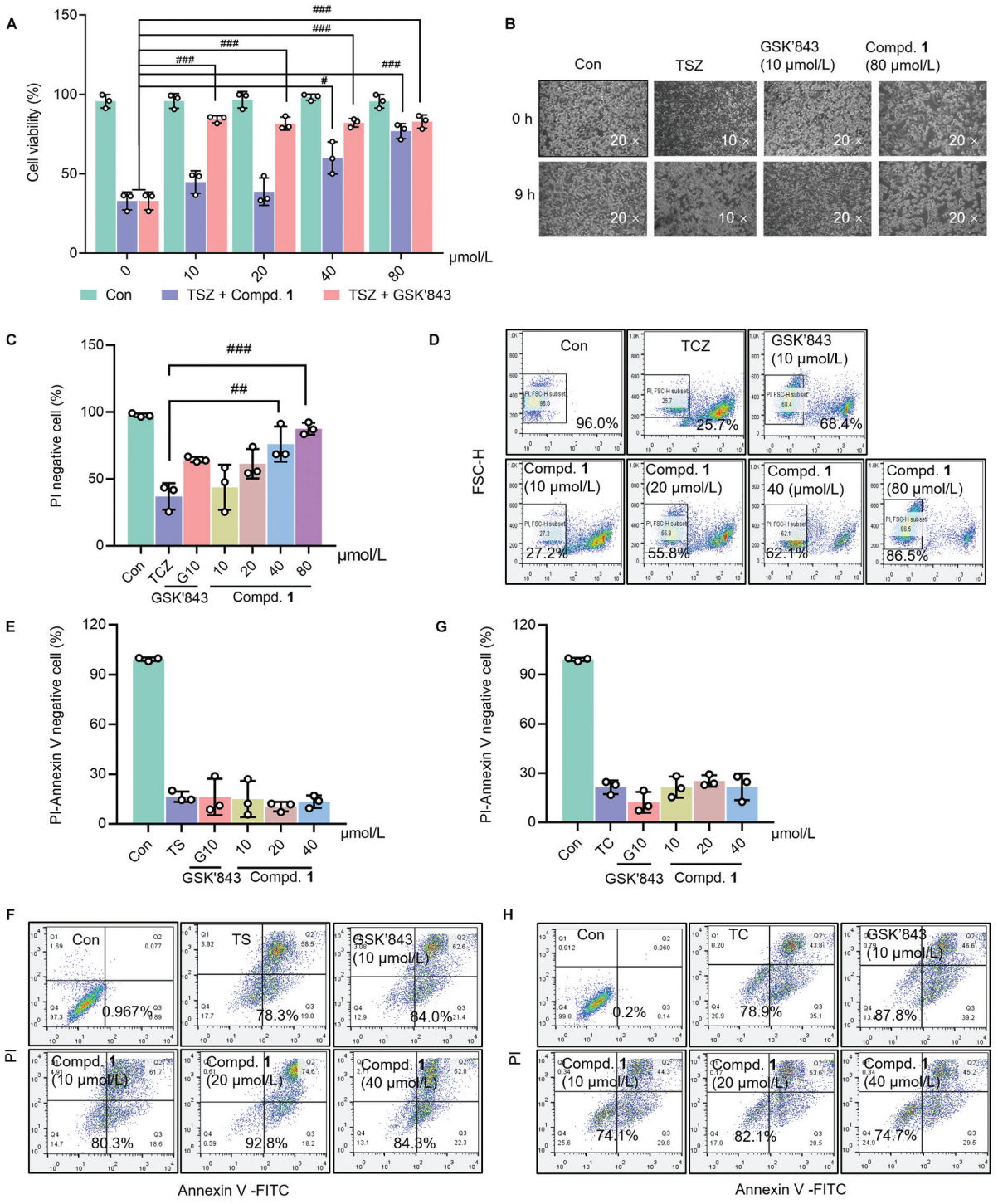

Fig. 3 The anti-necroptosis potency of compound **1** *in vitro*. (**A**) HT-29 cells were pretreated with compound **1** (10, 20, 40, 80 μmol/L) and GSK'843 (10 μmol/L) and then exposed to TSZ for 9 hours; the proportion of PI-negative cells was subsequently assessed using flow cytometry with PI staining. (**B**) Representative image (magnification ×10 or ×20) of HT-29 cells pretreated with compound **1** (80 μmol/L) and GSK'843 (10 μmol/L), and subsequently stimulated with TSZ for 9 hours. (**C, D**) HT-29 cells were subjected to pretreatment with compound **1** at a range of concentrations (10, 20, 40 μmol/L) and GSK'843 at 10 μmol/L for 30 minutes followed by stimulation with TCZ for 12 hours, then stained with PI, and PI-negative cells were recorded by flow cytometry. (**E, F**) HT-29 cells were pretreated with compound **1** at different concentrations (10, 20, and 40 μmol/L) and GSK'843 at 10 μmol/L for 30 minutes followed by stimulation with TS or (**G, H**) TC for 24 hours, then stained by the Annexin V-FITC/PI Apoptosis Kit, and Annexin V-FITC(−)/PI(−) cells were recorded by flow cytometry. $^{\#}p < 0.05$, $^{\#\#}p < 0.01$, $^{\#\#\#}p < 0.001$ versus stimulation without compound **1**. PI, propidium iodide.

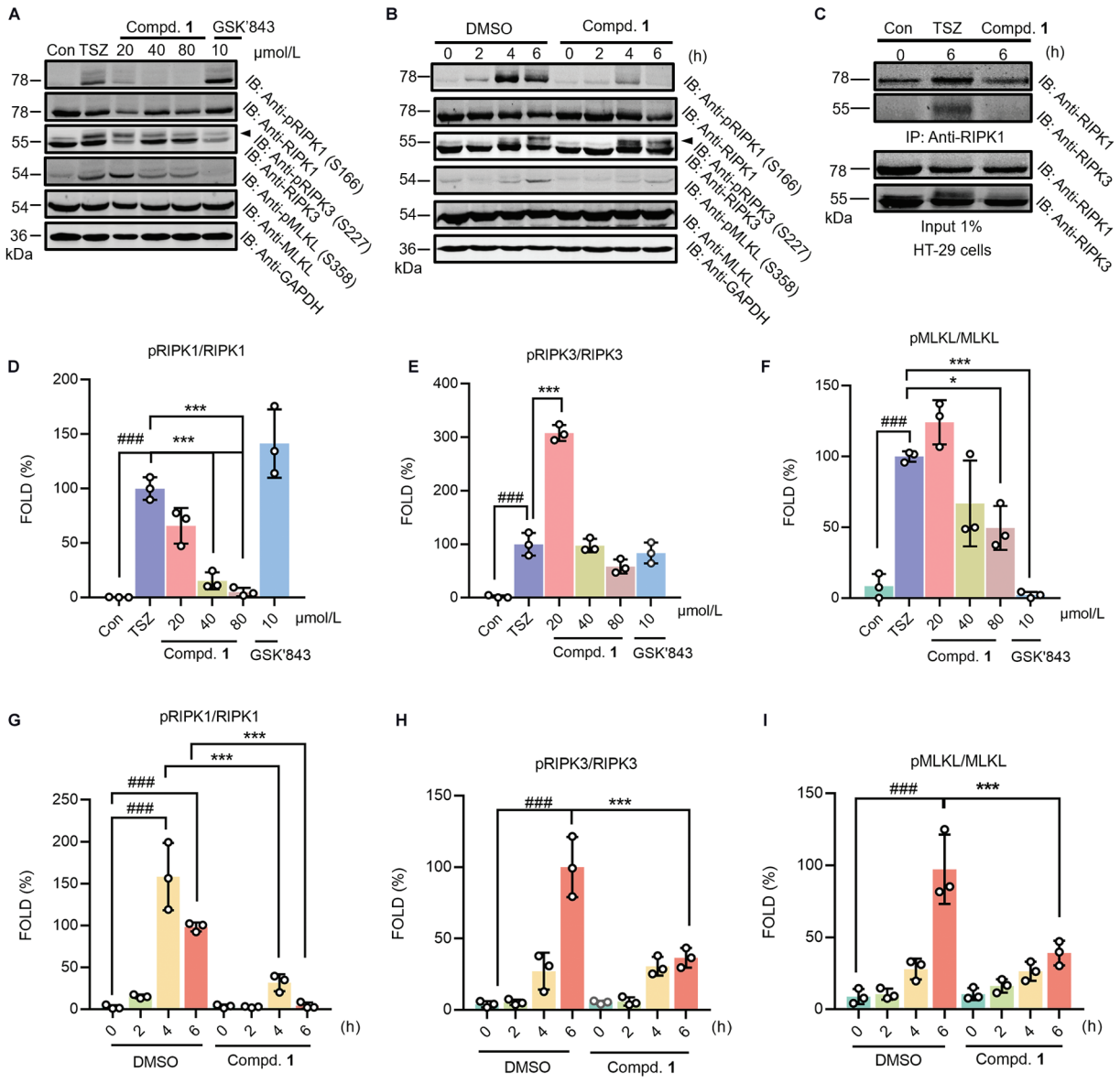

Fig. 4 Compound **1** blocked necroptosis through the inhibition of RIPK1 phosphorylation. (**A**) HT-29 cells were pretreated with compound **1** at specified concentrations (20, 40, and 80 μmol/L) and GSK'843 (10 μmol/L) for 30 minutes before a 6-hour exposure to TSZ. Cells were lysed, and the resulting lysates were analyzed by immunoblotting with the corresponding antibodies. (**B**) HT-29 cells were pretreated with DMSO or compound **1** at 80 μmol/L for 30 minutes followed by stimulation with TSZ at the specified time points. Immunoblotting was performed using the indicated antibodies after cell lysis. (**C**) HT-29 cells were pretreated with DMSO or compound **1** (80 μmol/L) and stimulated with TSZ for 6 hours. The cell lysates were subjected to immunoprecipitation using an anti-RIPK1 antibody (IP: RIPK1), followed by analysis through immunoblotting with specified antibodies. (**D–F**) Densitometric quantification of pRIPK1, pRIPK3, and pMLKL was performed across three independent dose-dependent experiments ($^{###}p < 0.001$ versus control, $^{*}p < 0.05$, $^{***}p < 0.001$ versus stimulation without compound **1**). (**G–I**) Densitometric quantification of pRIPK1, pRIPK3, and pMLKL was performed across three time-dependent independent assays ($^{###}p < 0.001$ versus control, $^{***}p < 0.001$ versus stimulation without compound **1**). FOLDS% represents the ratio of the gray values of phosphorylated RIPK1, phosphorylated RIPK3, and phosphorylated MLKL to the gray values of the individual total proteins, such as pRIPK1/RIPK1, pRIPK3/RIPK3, and pMLKL/MLKL.

anti-necroptosis therapeutics is of significant importance. In our experiments, we conducted a screening campaign using our in-house compound library to discover new chemotypes of necroptosis inhibitors. This led to the identification of compound **1**. Benzimidazole, a heterocyclic compound with a wide range of therapeutic effects, serves as a key pharmacophore in drug discovery.[41,42] Various benzimidazole derivatives have been recognized for their substantial biological efficacy, such as their antitumor,[43] antimicrobial,[44] antioxidant,[45] and anti-inflammatory properties.[46] Compound **1**, being a benzimidazole derivative, possesses a unique scaffold compared with previous necroptosis inhibitors, suggesting its potential for further development. We observed that i.p. administration of compound **1** provided protection to mice from TNF-induced SIRS *in vivo*.

However, several critical considerations should be taken into account regarding the *in vivo* application of compound **1**

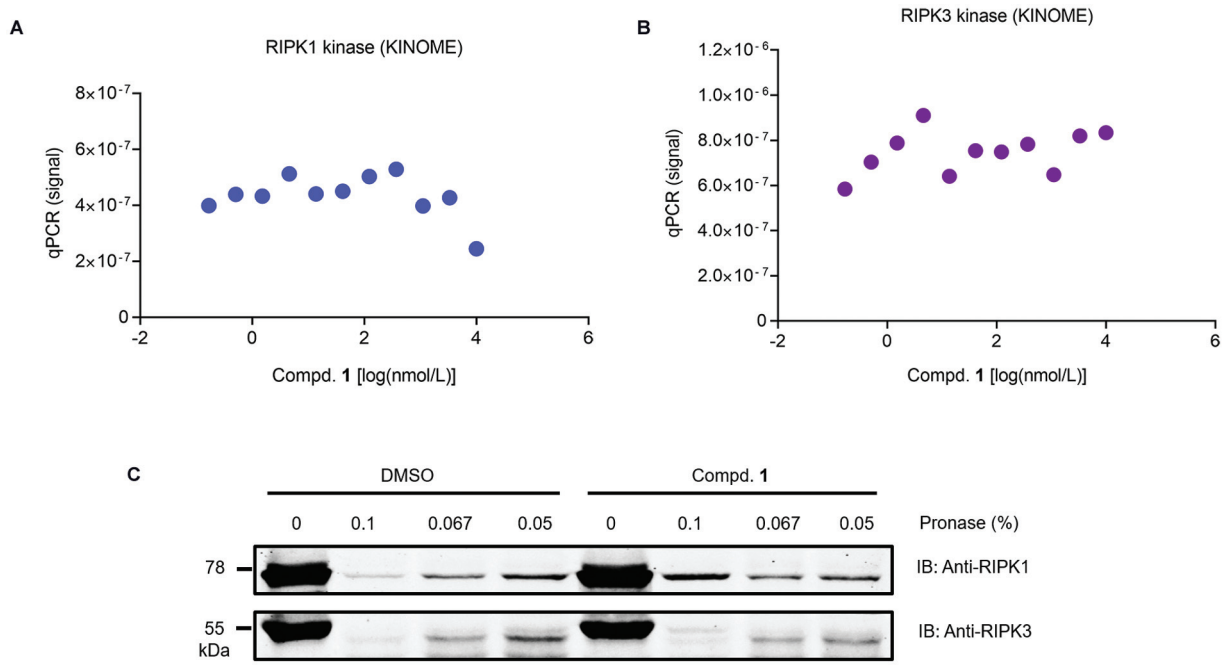

Fig. 5 Compound **1** inhibited necroptosis through the non-kinase domain of RIPK1. The inhibitory effects of compound **1** on (**A**) RIPK1 and (**B**) RIPK3 kinase activities, determined by the KINOMEscan assay. (**C**) Results from the DARTS assay. HT-29 cell lysates were exposed to DMSO or compound **1** (300 µmol/L) for 2 hours at 4°C followed by digestion with the indicated concentration of pronase at room temperature for 30 minutes and subsequently analyzed via immunoblotting with indicated antibodies.

as a necroptosis inhibitor. First, compound **1** displayed relatively low anti-necroptosis activity, necessitating a concentration of 80 µmol/L to achieve significant effects (►**Fig. 3A**, **C**). This could be due to its limited kinase activity. Second, while compound **1** was able to completely inhibit the phosphorylation of RIPK1 (S166) at 40 µmol/L in the necroptosis signaling pathway triggered by TNFα (►**Fig. 4A**, **B**), it did not fully block the phosphorylation of downstream substrates RIPK3 and MLKL (►**Fig. 4A**, **B**). Investigating the underlying mechanisms and the precise interaction site between compound **1** and RIPK1 will enhance our understanding of TNFα-induced necroptosis signaling pathways. In the SIRS model, oral administration of compound **1** did not protect mice from mortality (this is based on our preliminary experimental data, which has not been shown at present). Monitoring the metabolites following oral absorption could provide valuable insights for further investigation. Although compound **1** exhibited low RIPK1 kinase inhibitory activity, DARTS experiments indicated its interaction with RIPK1. Determining the exact target of compound **1** could be explored by transfecting different segments of recombinant truncated forms of RIPK1 in future studies.

Conclusion

Numerous necroptosis-inhibiting compounds, designed to ltarget key elements of necroptosis such as RIPK1, RIPK3, and MLKL, have been developed. Several of these have progressed to clinical trials, but none have yet been used in clinical trials.[26] In this study, we screened our proprietary compound library and identified compound **1** as a potential new inhibitor of necroptosis. Compound **1** was able to protect HT-29 cells from TSZ- or TCZ-induced necroptosis but not apoptosis. It blocked necroptotic cell death by inhibiting serine/threonine phosphorylation on RIPK1, which subsequently suppressed the phosphorylation of RIPK3 and MLKL. Notably, this compound demonstrated high efficacy in preventing TNFα-induced hypothermia in murine models. In summary, the benzimidazole compound could serve as a lead compound for further optimization to develop novel anti-necroptosis agents.

Supporting Information

Detailed information for the Western blot demonstrating the repeated runs for ►**Fig. 4A** and ►**Fig. 4B** (►**Fig. S1**, available in the online version), ^{1}H NMR and MS spectrum of compound **1** (►**Figs. S2** and **S3**, available in the online version), as well as the magnification of the TSZ group in ►**Fig. 3B** (►**Fig. S4**, available in the online version), is included in the Supporting Information.

Ethical Approval

All aspects of animal care and the experimental protocols adhered to the guidelines established by the National Institutes of Health and were approved by the Animal Care and Use Committee at the Second Military Medical University.

Funding

This research was financially supported by the National Natural Science Foundation of China (Grant No. 82022065) and the Science and Technology Commission of Shanghai Municipality (Grant No. 21S11900800).

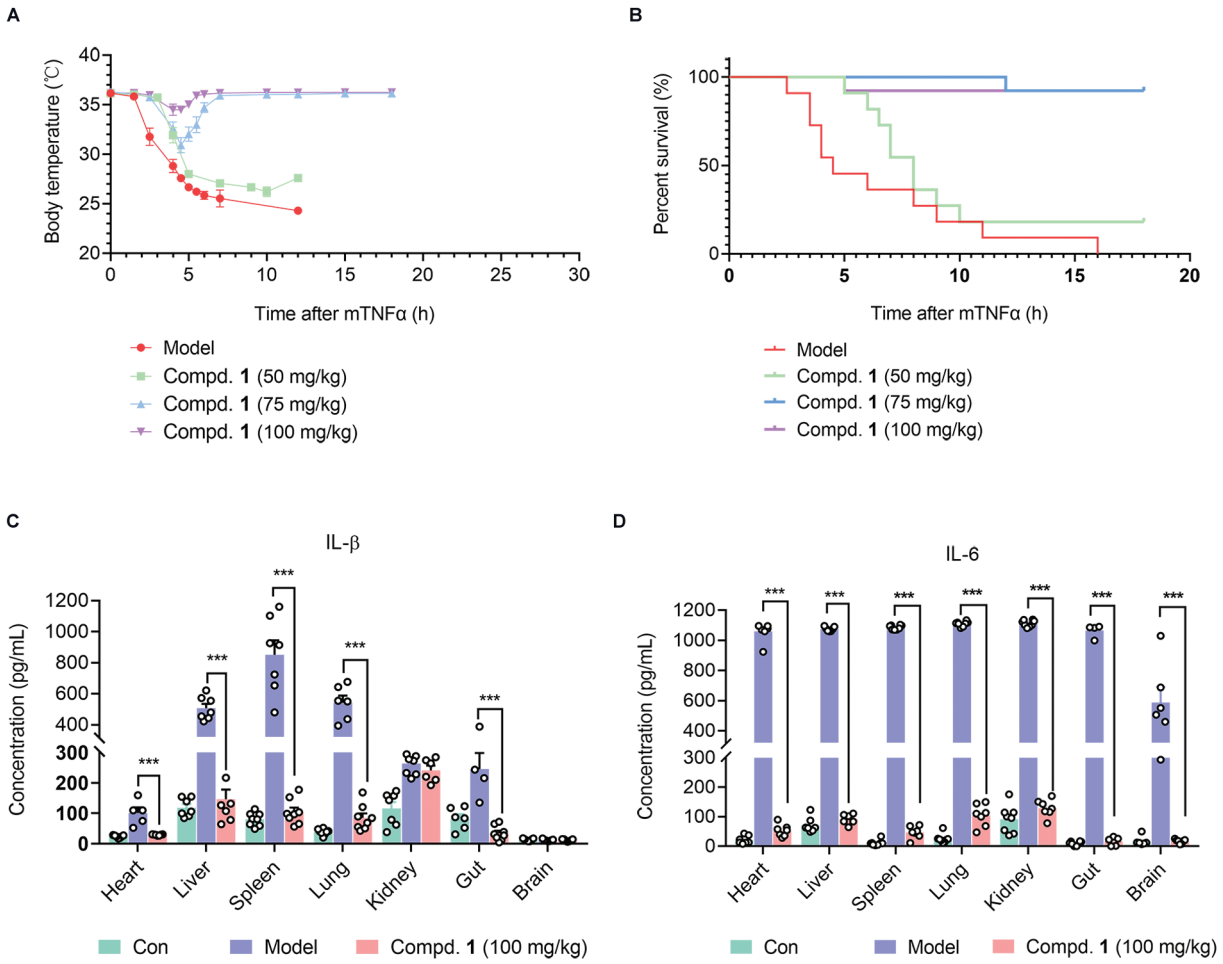

Fig. 6 Compound **1** alleviated the effects of TNF-induced SIRS in mice. (**A**) The body temperature (means ± SD) of C57BL/6 J male mice underwent pretreatment with or without compound **1** at various concentrations (100, 75, and 50 mg/kg), followed by the induction of SIRS using mouse TNFα (mTNFα) at a dosage of 50 μg/kg and Z-VAD-FMK at 200 μg/kg. (**B**) The survival rate of mice in the vehicle control and compound **1**-treated groups ($n = 12$). (**C**) Following an 8-hour post-SIRS induction, the levels of (**C**) IL-1β and (**D**) IL-6 in the respective tissues were quantified using an ELISA Kit. $^{***}p < 0.001$ versus the vehicle control group. SIRS, systemic inflammatory response syndrome; TNF, tumor necrosis factor.

Conflict of Interest

None declared.

References

1 Pasparakis M, Vandenabeele P. Necroptosis and its role in inflammation. Nature 2015;517(7534):311–320
2 Magnusson C, Vaux DL. Signalling by CD95 and TNF receptors: not only life and death. Immunol Cell Biol 1999;77(01):41–46
3 Kaiser WJ, Sridharan H, Huang C, et al. Toll-like receptor 3-mediated necrosis via TRIF, RIP3, and MLKL. J Biol Chem 2013; 288(43):31268–31279
4 Ingram JP, Thapa RJ, Fisher A, et al. ZBP1/DAI drives RIPK3-mediated cell death induced by IFNs in the absence of RIPK1. J Immunol 2019;203(05):1348–1355
5 Vanden Berghe T, Linkermann A, Jouan-Lanhouet S, Walczak H, Vandenabeele P. Regulated necrosis: the expanding network of non-apoptotic cell death pathways. Nat Rev Mol Cell Biol 2014;15 (02):135–147
6 Sarhan M, Land WG, Tonnus W, Hugo CP, Linkermann A. Origin and consequences of necroinflammation. Physiol Rev 2018;98 (02):727–780
7 Galluzzi L, Kepp O, Chan FK, Kroemer G. Necroptosis: mechanisms and relevance to disease. Annu Rev Pathol 2017;12:103–130
8 Chen G, Goeddel DV. TNF-R1 signaling: a beautiful pathway. Science 2002;296(5573):1634–1635
9 Wajant H, Pfizenmaier K, Scheurich P. Tumor necrosis factor signaling. Cell Death Differ 2003;10(01):45–65
10 Christofferson DE, Li Y, Yuan J. Control of life-or-death decisions by RIP1 kinase. Annu Rev Physiol 2014;76:129–150
11 Micheau O, Tschopp J. Induction of TNF receptor I-mediated apoptosis via two sequential signaling complexes. Cell 2003; 114(02):181–190
12 O'Donnell MA, Perez-Jimenez E, Oberst A, et al. Caspase 8 inhibits programmed necrosis by processing CYLD. Nat Cell Biol 2011;13 (12):1437–1442
13 Feng S, Yang Y, Mei Y, et al. Cleavage of RIP3 inactivates its caspase-independent apoptosis pathway by removal of kinase domain. Cell Signal 2007;19(10):2056–2067
14 Cho YS, Challa S, Moquin D, et al. Phosphorylation-driven assembly of the RIP1-RIP3 complex regulates programmed necrosis and virus-induced inflammation. Cell 2009;137(06):1112–1123
15 Li J, McQuade T, Siemer AB, et al. The RIP1/RIP3 necrosome forms a functional amyloid signaling complex required for programmed necrosis. Cell 2012;150(02):339–350
16 Sun L, Wang H, Wang Z, et al. Mixed lineage kinase domain-like protein mediates necrosis signaling downstream of RIP3 kinase. Cell 2012;148(1–2):213–227

17 Chen W, Zhou Z, Li L, et al. Diverse sequence determinants control human and mouse receptor interacting protein 3 (RIP3) and mixed lineage kinase domain-like (MLKL) interaction in necroptotic signaling. J Biol Chem 2013;288(23):16247–16261
18 Cai Z, Jitkaew S, Zhao J, et al. Plasma membrane translocation of trimerized MLKL protein is required for TNF-induced necroptosis. Nat Cell Biol 2014;16(01):55–65
19 Wang H, Sun L, Su L, et al. Mixed lineage kinase domain-like protein MLKL causes necrotic membrane disruption upon phosphorylation by RIP3. Mol Cell 2014;54(01):133–146
20 Berger SB, Kasparcova V, Hoffman S, et al. Cutting Edge: RIP1 kinase activity is dispensable for normal development but is a key regulator of inflammation in SHARPIN-deficient mice. J Immunol 2014;192(12):5476–5480
21 Degterev A, Huang Z, Boyce M, et al. Addendum: Chemical inhibitor of nonapoptotic cell death with therapeutic potential for ischemic brain injury. Nat Chem Biol 2013;9(03):192
22 Takahashi N, Duprez L, Grootjans S, et al. Necrostatin-1 analogues: critical issues on the specificity, activity and in vivo use in experimental disease models. Cell Death Dis 2012;3(11):e437
23 Ren Y, Su Y, Sun L, et al. Discovery of a highly potent, selective, and metabolically stable inhibitor of receptor-interacting protein 1 (RIP1) for the treatment of systemic inflammatory response syndrome. J Med Chem 2017;60(03):972–986
24 Berger SB, Harris P, Nagilla R, et al. Characterization of GSK'963: a structurally distinct, potent and selective inhibitor of RIP1 kinase. Cell Death Discov 2015;1:15009
25 Harris PA, Faucher N, George N, et al. Discovery and lead-optimization of 4,5-dihydropyrazoles as mono-kinase selective, orally bioavailable and efficacious inhibitors of receptor interacting protein 1 (RIP1) kinase. J Med Chem 2019;62(10):5096–5110
26 Harris PA, Berger SB, Jeong JU, et al. Discovery of a first-in-class receptor interacting protein 1 (RIP1) kinase specific clinical candidate (GSK2982772) for the treatment of inflammatory diseases. J Med Chem 2017;60(04):1247–1261
27 Yoshikawa M, Saitoh M, Katoh T, et al. Discovery of 7-Oxo-2,4,5,7-tetrahydro-6*H*-pyrazolo[3,4-*c*]pyridine derivatives as potent, orally available, and brain-penetrating receptor interacting protein 1 (RIP1) kinase inhibitors: analysis of structure-kinetic relationships. J Med Chem 2018;61(06):2384–2409
28 Vissers MFJM, Heuberger JAAC, Groeneveld GJ, et al. Safety, pharmacokinetics and target engagement of novel RIPK1 inhibitor SAR443060 (DNL747) for neurodegenerative disorders: randomized, placebo-controlled, double-blind phase I/Ib studies in healthy subjects and patients. Clin Transl Sci 2022;15(08):2010–2023
29 Mandal P, Berger SB, Pillay S, et al. RIP3 induces apoptosis independent of pronecrotic kinase activity. Mol Cell 2014;56(04):481–495
30 Chen X, Zhuang C, Ren Y, et al. Identification of the Raf kinase inhibitor TAK-632 and its analogues as potent inhibitors of necroptosis by targeting RIPK1 and RIPK3. Br J Pharmacol 2019;176(12):2095–2108
31 Zhu J, Qu Z, Huang J, et al. Enantiomeric profiling of a chiral benzothiazole necroptosis inhibitor. Bioorg Med Chem Lett 2021;43:128084
32 Zhang X, Han Q, Hou R, et al. Targeting receptor-interacting protein kinase 1 by novel benzothiazole derivatives: treatment of acute lung injury through the necroptosis pathway. J Med Chem 2023;66(07):5261–5278
33 Zhang H, Xu L, Qin X, et al. *N*-(7-Cyano-6-(4-fluoro-3-(2-(3-(trifluoromethyl)phenyl)acetamido)phenoxy)benzo[*d*]thiazol-2-yl)cyclopropanecarboxamide (TAK-632) analogues as novel necroptosis inhibitors by targeting receptor-interacting protein kinase 3 (RIPK3): synthesis, structure-activity relationships, and in vivo efficacy. J Med Chem 2019;62(14):6665–6681
34 Zhu J, Xin M, Xu C, et al. Ligand-based substituent-anchoring design of selective receptor-interacting protein kinase 1 necroptosis inhibitors for ulcerative colitis therapy. Acta Pharm Sin B 2021;11(10):3193–3205
35 Xu Y, Liang C, Zhang W, et al. Profiling of the chemical space on the phenyl group of substituted benzothiazole RIPK3 inhibitors. Bioorg Chem 2023;131:106339
36 Xu L, Tu Y, Li J, et al. Structure-based optimizations of a necroptosis inhibitor (SZM594) as novel protective agents of acute lung injury. Chin Chem Lett 2022;33(05):2545–2549
37 Hao Y, Shao H, Qu Z, et al. Investigation on the chemical space of the substituted triazole thio-benzoxazepinone RIPK1 inhibitors. Eur J Med Chem 2022;236:114345
38 Lomenick B, Hao R, Jonai N, et al. Target identification using drug affinity responsive target stability (DARTS). Proc Natl Acad Sci U S A 2009;106(51):21984–21989
39 Fang JJ, Yao HZ, Zhuang C, Chen FE. Insight from linker investigations: discovery of a novel phenylbenzothiazole necroptosis inhibitor targeting receptor-interacting protein kinase 1 (RIPK1) from a phenoxybenzothiazole compound with dual RIPK1/3 targeting activity. J Med Chem 2023;66(22):15288–15308
40 Quan D, Hou R, Shao H, et al. Structure-based design of novel alkynyl thio-benzoxazepinone receptor-interacting protein kinase-1 inhibitors: extending the chemical space from the allosteric to ATP binding pockets. J Med Chem 2023;66(04):3073–3087
41 Keri RS, Hiremathad A, Budagumpi S, Nagaraja BM. Comprehensive review in current developments of benzimidazole-based medicinal chemistry. Chem Biol Drug Des 2015;86(01):19–65
42 Yadav G, Ganguly S. Structure activity relationship (SAR) study of benzimidazole scaffold for different biological activities: A mini-review. Eur J Med Chem 2015;97:419–443
43 Gowda NR, Kavitha CV, Chiruvella KK, Joy O, Rangappa KS, Raghavan SC. Synthesis and biological evaluation of novel 1-(4-methoxyphenethyl)-1*H*-benzimidazole-5-carboxylic acid derivatives and their precursors as antileukemic agents. Bioorg Med Chem Lett 2009;19(16):4594–4600
44 Kumar BV, Vaidya SD, Kumar RV, Bhirud SB, Mane RB. Synthesis and anti-bacterial activity of some novel 2-(6-fluorochroman-2-yl)-1-alkyl/acyl/aroyl-1*H*-benzimidazoles. Eur J Med Chem 2006;41(05):599–604
45 Dvornikova IA, Buravlev EV, Fedorova IV, Shevchenko OG, Chukicheva IY, Kutchin AV. Synthesis and antioxidant properties of benzimidazole derivatives with isobornylphenol fragments. Russ Chem Bull 2019;68(05):1000–1005
46 Gaba M, Gaba P, Uppal D, et al. Benzimidazole derivatives: search for GI-friendly anti-inflammatory analgesic agents. Acta Pharm Sin B 2015;5(04):337–342

